Molecular Crystals and Liquid Crystals

Publication details, including instructions for authors and subscription information:
http://www.tandfonline.com/loi/gmcl20

Local Three-Dimensional Characterization of a Micro-Patterned Liquid Crystalline Cell by Confocal Raman Microscopy

P. Camorani [a] & M. P. Fontana [a]

[a] Physics Department, University of Parma, INFM-CNR CRS Soft

Version of record first published: 22 Sep 2010

To cite this article: P. Camorani & M. P. Fontana (2007): Local Three-Dimensional Characterization of a Micro-Patterned Liquid Crystalline Cell by Confocal Raman Microscopy, Molecular Crystals and Liquid Crystals, 465:1, 143-152

To link to this article: http://dx.doi.org/10.1080/15421400701205719

Mol. Cryst. Liq. Cryst., Vol. 465, pp. 143–152, 2007

ISSN: 1542-1406 print/1563-5287 online
DOI: 10.1080/15421400701205719

Taylor & Francis
Taylor & Francis Group

Local Three-Dimensional Characterization of a Micro-Patterned Liquid Crystalline Cell by Confocal Raman Microscopy

P. Camorani
M. P. Fontana
Physics Department, University of Parma, INFM-CNR CRS Soft

We present an experimental study on the local liquid crystalline alignment in a dye-doped nematic cell with an optically micropatterned command surface. The experiments have been carried out on cells filled with pentyl-cyanobiphenyl (5CB) doped with azo dyes with a wall coated with polyvinylcinnamate-fluorinated (PVCN-F) acting as command surface. The microstructures have been produced trough an anisotropic light-induced adsorption of the azo dyes on the command surface and the subsequent reorientation of the nematic axis at the interface and its propagation inside the cell has been characterized by confocal polarized micro Raman spectroscopy. Both lateral and axial profiles of nematic director and order parameter have been measured providing a 3D visualization of the microstructures. Particular attention has been given to the solid-liquid crystal interactions and their influences on the bulk liquid crystalline order.

Keywords: confocal polarized Raman spectroscopy; 3D imaging; azo dyes; liquid crystals

INTRODUCTION

Three dimensional visualization of the molecular orientation and order parameter has always been a fundamental issue in liquid crystals physics. For such a task confocal microscopy may represent a unique tool.

Other techniques have been applied to obtain nanometer resolution separately for planar and Z (off-plane) direction: the surface can be

We are grateful to Prof. O. Francescangeli and Dr. L. Lucchetti for providing us the know-how and the materials for the sample preparation in addition to assembled cells. We wish to thank Prof. L. Cristofolini for useful discussions. This work has been financially supported by INFM (PAIS LIMAD project) and INFM-CNR CRS Soft.

Address correspondence to P. Camorani, Physics Department, University of Parma, INFM-CNR CRS Soft. E-mail: paolo.camorani@fis.unipr.it

characterized using scanning probe techniques such as scanning near field optical microscopy (SNOM) for birefringence [1] and optical dichroism [2] measurements or lateral force microscopy (LFM) for the easy axis determination by tribology [3], while the z-direction profiles of a liquid crystal cell can be characterized with ellipsometric techniques such as half-leaky guided mode (HLGM)[4]. Confocal microscopy providing features at sub-μm resolution both in plane and off-plane of the samples, allows the simultaneous three dimensional approach. Up to now such technique has been applied to liquid crystals using fluorescence contrast [5], by dispersing fluorescent dyes in the liquid crystalline host, while so far Raman contrast has been used to characterize z profile of a bent nematic cell [6] and the plane projection of the configuration a Polymer Dispersed Liquid Crystal PDLC droplet [7]. Here we present a characterization of a 3D micrometric structure.

Polarized Raman spectroscopy [8], as polarized fluorescence [9], are well established techniques for measuring the order parameter and orientation in liquid crystals. Raman spectroscopy, despite its lower cross section, presents two main advantages: it measures the signal directly from the molecules under study without need of probes and may provide a chemical contrast in a multicomponent system. The totally symmetric strongly uniaxial vibrations of the phenyl moiety for example, present in many mesogenic compounds, provide a suitable Raman probe for the orientation measurement. A common drawback of all techniques requiring a probe is that their molecular structure must match the host one, to assure that the guest reflects the behavior of the matrix under investigation as closely as possible. The second advantage of Raman spectroscopy is the chemical contrast, which may be of special interest in a multi compound system as most of the modern devices are. For example in the particular system subject of this work, an azo dye doped liquid crystal, we could resolve both dynamics and spatial distribution of doping dye and liquid crystal matrix using a dye with a suitable Raman active group [10].

MATERIAL AND METHODS

The system studied is a liquid crystalline cell filled with a low molecular weight dye doped liquid crystal assembled using two different boundary glass walls: an aligning *reference* surface and an isotropic *command* surface. The reference substrate was coated with a polyimide layer mechanically rubbed in order to obtain a strong homogeneous planar orientation while second surface was coated with a layer of fluorinated polyvinyl-cinnamate (PVCN-F) cured with

unpolarized UV light, which provides a degenerate planar anchoring with negligible azimuthal component.

The cell was filled with a mixture of the commercial nematic liquid crystal pentyl-cyanobiphenyl (5CB) and the azo-dye Methyl Red (MR) at 0.5% weight concentration. In such system the anchoring conditions of the command surface can be controlled by a photoinduced adsorption/desorption of the MR dopant [10,11], in particular illumination with polarized light induces an anisotropic concetration of the mesogenic MR molecules on the command substrate with a consequent easy axis reorientation of the 5CB at the interface. Twisted structures can be obtained by photoadsorption of the MR on the command surface perpendicularly to the rubbing direction of the reference surface as shown in cell scheme in Figure 1.

We produced such twisted microstructures in the cell trough a confocal illumination on PVCN-F surface with the 488 nm Ar/Kr^{+} laser line and then proceeded with the characterization using the same confocal microscope with a different laser line at 647 nm, wavelength which is outside the MR absorption band. Raman spectra were collected in the back scattering geometry with a Jobin Yvon-Horiba T64000 microspectrometer equipped with a liquid N_2 cooled CCD detector. The depolarized Raman signal was acquired also during the writing process in order to monitor the microstructure formation. The use of

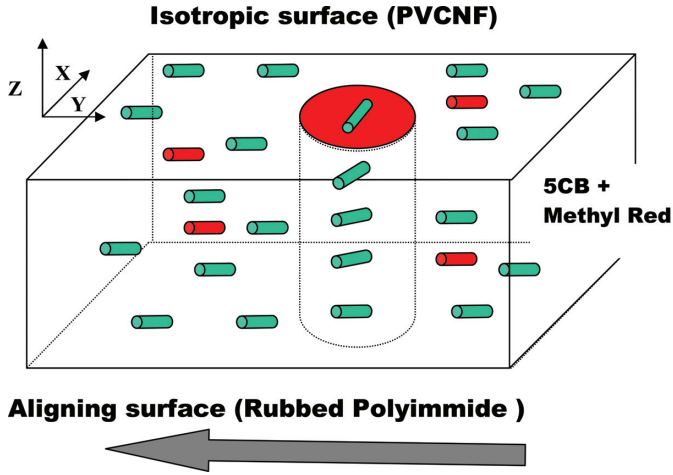

FIGURE 1 Scheme of the liquid crystalline cell: command surface on top, aligning surface on bottom. Illumination induces an easy axis reorientation on the command surface perpendicular to the cell axis, resulting in a 90 degree twisted structure. (See COLOR PLATE XI)

confocal illumination in this process, however, is unnecessary since we were unable to obtain structure smaller than 10 μm diameter which is plausibly a critical size due to the 5CB order correlation length and cell depth (≈15 μm). The spatial resolution obtainable instead for characterization, in the micro-Raman set up, is diffraction limited to the values of 0.61 λ/NA and 1.4 $\lambda\ n/(\mathrm{NA})^2$ respectively for the lateral and the axial resolution, where λ is the excitation wavelength, NA the numerical aperture of the objective, and n its refractive index of the medium. Using as in our case, a laser excitation wavelength of 647 nm of the Ar/Kr^+ line and a 100× oil (n = 1.45) immersion with NA = 1.3, we obtain theoretical lateral and axial resolutions of 0.3 and 0.7 μm, respectively. An accurate calibration of both polarization response and extinction ratio of the instrument has been made using a CCl_4 solution according to Ref. [13].

The polarized micro-Raman study has been carried out measuring the peaks intensities as a function of the incident polarization and the analyzer directions along the two orthogonal axis V and H, respectively parallel and perpendicular to the nematic director: the measurements were done on the four possible geometries 'VV','VH','HH','HV', where the first index refer to incident polarization and the second to the analyzer direction. The fist two order parameters P_2 and P_4 can be directly obtained on the basis of scattering anisotropies R_1 and R_2 defined as: $R_1 = \mathrm{I_{VH}}/\mathrm{I_{VV}}$, $R_2 = \mathrm{I_{HV}}/\mathrm{I_{HH}}$.

In particular if the considered molecular vibration has a strongly uniaxial polarizability tensor, related to the molecular frame, in the diagonal form:

$$\alpha = \begin{pmatrix} \alpha_H & 0 & 0 \\ 0 & \alpha_H & 0 \\ 0 & 0 & \alpha_V \end{pmatrix}$$

with $\alpha_H/\alpha_V \approx 0$ the order parameter P_2 and P_4 can be calculated from the second and fourth average cosine powers of the molecular orientation θ which may be written in the form:

$$\langle(\cos\theta)^2\rangle = \frac{3R_2(2R_1+1)}{8R_1+3R_2+12R_1R_2} \tag{1}$$

$$\langle(\cos\theta)^4\rangle = \frac{3R_2}{8R_1+3R_2+12R_1R_2} \tag{2}$$

RESULTS

We measured the order parameter on the three different surfaces of our system namely: reference surface, pristine and irradiated command surface.

In our notation we indicate with x, y, z the three axes of the cell, with the y axis along the rubbing direction ad z normal to the surface. For sake of clarity we recall the correspondence with the direction V of the nematic axis defined in the previous section: it corresponds to the y axis in the pristine planar cell or to the x axis in the irradiated area on the command surface. In Figure 2 are reported the Raman intensities I_{ij} where i and j indicate the incoming polarization and the analyzer directions acquired on the command surface in the irradiated and non-irradiated area. The spectra measured on the reference surface are not shown since they are qualitatively equivalent to those obtained on the pristine command surface. The spectra show the four characteristic peaks of 5CB namely: the 1208 cm^{-1} benzene vibration, the stretching of the biphenyl link (1314 cm^{-1}), the symmetric stretching of the benzene rings (1605 cm^{-1}) and stretching of the CN cyano group (2258 cm^{-1}). Since the intensity of scattered Raman radiation depends on the square of the oscillating induced dipole, the Raman intensity is greater for illumination with polarization along α_V than along α_H direction. The axis of α_v is that at which the maximum Raman signal occurs. The intensity of the signal indicates the perpendicular orientation of the nematic director on the two probed areas of the surface, the total Raman signal is higher if the electric vector of the incident beam lies along the cell y-axis in the unirradiated area and x for the illuminated one. All modes result polarized even if with a different degree; both cyano and the phenyl stretching can be used to characterize molecular alignment. Cyano stretch however is extremely sensitive to polarity, which may

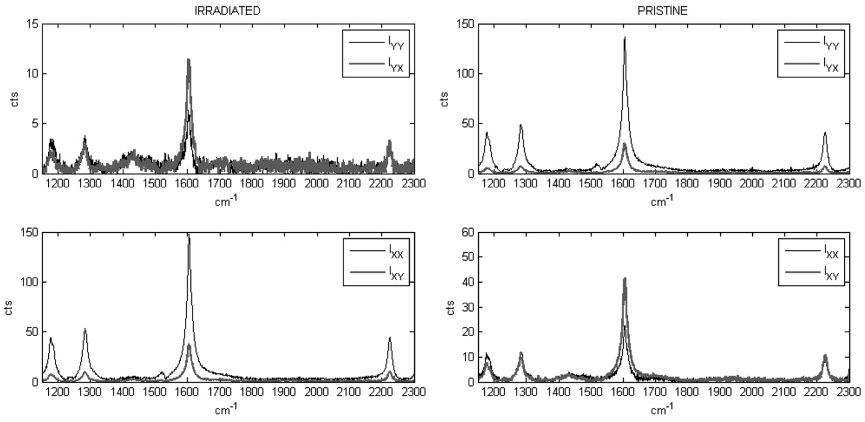

FIGURE 2 Polarized Raman spectra acquired on irradiated area (left graphs) and pristine surface (right). The exiting polarization lays in the y or x direction in upper and bottom plots respectively.

vary at the interface, and has been found to be slightly biaxial[14], moreover has a weaker signal respect to the benzene mode. Therefore in the present study, we investigated the mode at $1605\,cm^{-1}$, although this vibration is complex since it may be influenced by intermolecular interactions, the main axis of the vibration is parallel to the central, rigid part of the molecule, in other words, along the main axis of the mesogenic group. Such vibration is also particularly suitable since it is strongly polarized with a value $\alpha_H/\alpha_V = 0.045$, determined by scattering anisotropy measurements in the isotropic phase [15]. Such value close to zero allows us to use the approximate Eqs. (1) and (2) for the order parameters calculation. We applied such approximation also considering that it may cause a systematic underestimation of the order parameter which doesn't affect in any case the validity of our considerations.

The scattering anisotropies R_1 R_2 of the benzene mode measured on the three surfaces and the resulting order parameter P_2 are reported in Table 1.

Confocal Raman results therefore evidence the variations of the molecular alignment due to the different interface interactions. From our measurements the order results higher, as expected, on the reference surface, where there are strong anchoring conditions, while on the isotropic surface probably reflects the lower bulk value. Further investigation, extended to the bulk alignment, were performed measuring the depolarization anisotropy of the $1605\,cm^{-1}$mode along Z direction. In Figure 3 are shown the Raman signal profiles of the cell measured from the isotropic surfaces. The resolution of the setup can evaluated from the top plot reporting the total Raman intensity, it indicates a higher resolution (around $2\,\mu m$) on the first encountered interface where the signal increases steeply. On the second surface instead, the resolution is degraded by a factor 2, in this case the signal is probably affected by the scattering coming from the entire cell crossed by the laser beam probe. The ratio between the two polarization components (bottom and middle panel Figure 3 respectively) shows a constant value of $R_1 \approx 0.26$ along the cell profile, the scattering of points outside the cell wall, reflects the noise of data obtained by a ratio between two low

TABLE 1 Scattering Anisotropies R_1 and R_2 and order Parameters P_2 on the Different System Surfaces

	R_1 (± 0.005)	R_2 (± 0.02)	P_2 (± 0.01)
Aligning surface	0.182	1.7	0.52
Isotropic surface before irradiation	0.262	1.96	0.45
Isotropic surface after irradiation	0.219	1.89	0.48

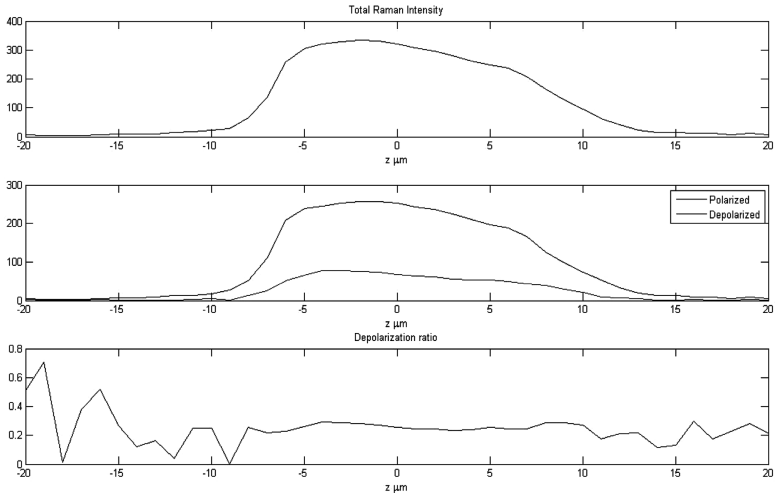

FIGURE 3 Intensity of the $1605\,cm^{-1}$ mode along Z direction of the cell measured from the command surface. Top panel shows the total intensity, middle panel the polarization components and depolarization ratio in the lower one. (cell boundaries at $z_1 \approx -6\,\mu m$ and $z_2 \approx 9\,\mu m$).

intensities. The measured anisotropy R_1 which is plausibly constant on the isotropic surface and in bulk, however doesn't agree on the bottom surface with the previously measured value (0.18 reported in Table 1). Such fact suggests that depolarization profiles should be measured in both directions and compared. On Figure 4 are shown the profiles measured, starting from the aligning surface, on the lower left graph are reported the profiles measured on planar zone of the cell while on the right those in the photoinduced twist structure. The anisotropy R_1 in the pristine cell (bottom left Fig. 4) goes now from the value 0.18 on the aligning surface to 0.28 on the isotropic one, value also in this case higher than previously reported (0.26 reported in Table 1). By the comparison of the two measurements in the same zone we can conclude that scattering signal, taking place when the entire cell is crossed by the probe beam, induces an overestimation of the depolarization ratio, which may be taken into account by the bi-directional measurement. The variation of order parameter from interfaces to bulk can be evidenced however at the top surface, where spurious effects are negligible, in particular the last considered plot the value R_1 increases right after the aligning surface, indicating a deterioration of order in the bulk.

As to the confocal measurements in the irradiated area on the right plots of Figure 4, they reflect the created twisted structure: the relative inversion of the polarized and depolarized intensities (top

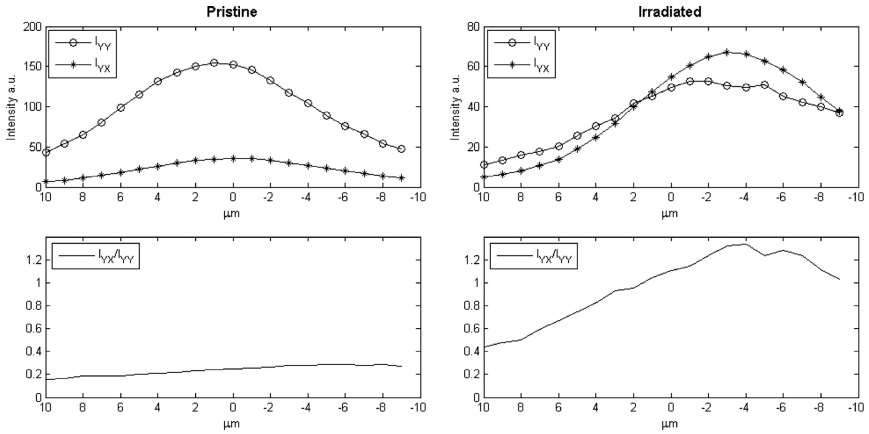

FIGURE 4 Polarization components (upper plots) and depolarization ratio (lower plots) of the 1605 cm^{-1} peak along Z direction. Measurements were performed from the command surface on the pristine cell (left plots) and on the irradiated region (right). (Cell boundaries at $z_1 \approx 8\,\mu m$ and $Z_2 \approx -8\,\mu m$.)

right graph on Fig. 4) indicates that the measured anisotropy (bottom right graph on Fig. 4) corresponds to the parameter R_1 on the top surface and to R_2 at the bottom, or in simpler words a 90 degree rotation of the director along the cell. The apparent decrease of the depolarization ratio on the bottom of the cell is probably due to the scattering contribution discussed above, as a matter of fact it doesn't appear in the same measurement performed from the opposite direction which is shown in the lower right graph in Figure 5.

Finally we performed a complete three dimensional characterization of a 10 μm diameter twisted structure whose section (which we show instead of a 3D representation for more readability and considering the axial symmetry) is reported in Figure 5. The top images report respectively the depolarized and polarized signal and their ratio in the lower left panel, visualizing the microstructure in the YZ dimensions. For completeness two profiles of anisotropy, inside and outside the twist structure, are shown in the lower right plot.

CONCLUSION AND FUTURE WORK

We applied confocal Raman micro spectrometry technique with polarization contrast to the study of a liquid crystalline system having different kind of cell surfaces, which in turn play a fundamental role in the potential application of the system in optical devices. In particular

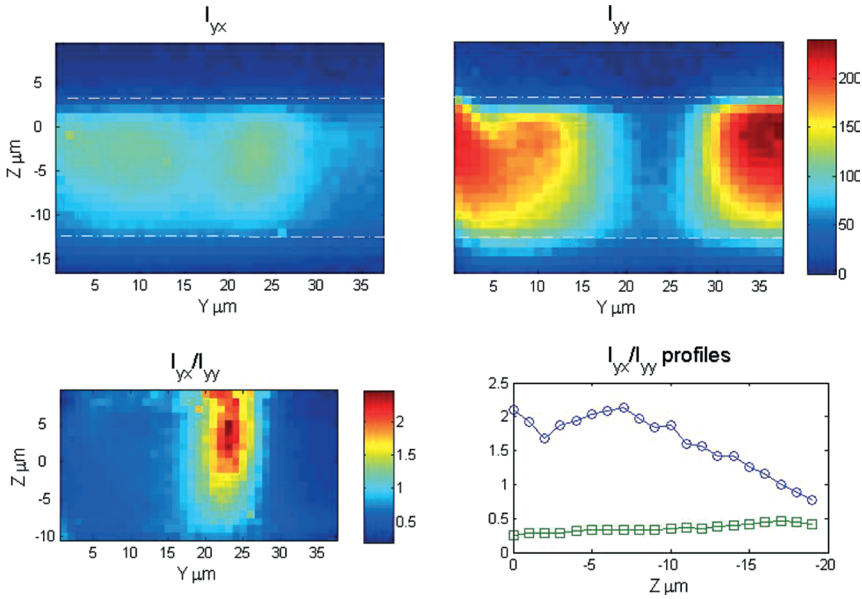

FIGURE 5 YZ sections of a 10 µm twisted structure. Depolarized and polarized raman signals are shown respectively on the left and right upper plots (cell boundaries marked with the dotted lines). Depolarization ratio is shown in the left bottom image. The right bottom graph reports the anisotropy profiles in the planar zone (circle) and in the twisted structure (squares), measured respectively at coordinates $y_1 = 30$ and $y_2 = 22\,\mu m$. (See COLOR PLATE XII)

we show how the technique is able to characterize the surface-liquid crystals interaction evidencing the differences between the interface and bulk liquid crystalline order. As second result we obtained a three dimensional visualization of molecular director of a micron size structure. Current effort focusses now on quantitative analysis the of anisotropy z-profiles with quantification of the spurious observed effects.

REFERENCES

[1] Reid, P. J., Higgins, D. A., & Barbara, P. F. (1996). *J. Phys. Chem.*, *100*, 3892.
[2] Lacoste, T., Huser, T., Prioli, R., & Heinzelmann, H. (1998). *Ultramicroscopy*, *71*, 333–340.
[3] Rüetschi, M., Fünfschilling, J., & Güntherodt, H.-J. (1996). *J. Appl. Phys.*, *80*, 3155.
[4] Yang, F. & Sambles, J. R. (1993). *J. Opt. Soc. Am. B*, *10*, 858; Mazzulla, A., Ciuchi, F., & Sambles, J. R. (2001). *Phys. Rev. E*, *64*, 021708.

[5] Smalyukh, I.I., Shiyanovskii, S. V., & Lavrentovich, O. (2001). *Chem. Phys. Lett.*, *336*(1–2), 88.
[6] Blach, J.-F., Warenghem, M., & Bormann, D. (2006). *Vib. Spectrosc.*, *41*(1), 48.
[7] Blach, J.-F., Daoudi, A., Buisine, J.-M., & Bormann, D. (2005). *Vib. Spectrosc.*, *39*(1), 31.
[8] Jen, S., Clark, N. A., Pershan, P. S., & Priestley, E. B. (1977). *J. Chem. Phys.*, *66*, 4635.
[9] Chapoy, L. L. & DuPre, D. B. (1979). *J. Chem. Phys.*, *70*, 2550.
[10] Camorani, P. & Fontana, M. P. manuscript in preparation.
[11] Francescangeli, O., Lucchetti, L., Simoni, F., Stanic, V., & Mazzulla, A. (2005). *Phys. Rev. E*, *71*, 011702.
[12] Fedorenko, D., Ouskova, E., Reshetnyak, V., & Reznikov, Y. (2006). *Phys. Rev. E*, *73*, 031701.
[13] Turrell, G. (1984). *J. Raman Spectrosc.*, *15*(2), 103.
[14] Miyano, K. (1978). *J. Chem. Phys.*, *69*(11), 4807.
[15] Bauman, D. (2005). *J. Mol. Struct.*, 744–747, 307.